Available online at www.sciencedirect.com
SCIENCE DIRECT®
Fluid Phase Equilibria 222–223 (2004) 149–159
FLUID PHASE EQUILIBRIA
www.elsevier.com/locate/fluid

Generalized crossover description of the thermodynamic and transport properties in pure fluids

S.B. Kiselev*, J.F. Ely

Chemical Engineering Department, Colorado School of Mines, Golden, CO 80401-1887, USA

Available online 24 July 2004

Abstract

We have developed a generalized cubic (GC) EOS for pure fluids, which incorporates non-analytic scaling laws in the critical region and in the limit $\rho \to 0$ is transformed into the ideal gas equation EOS. The GC EOS contains 10 adjustable parameters and reproduces the thermodynamic properties of pure fluids with high accuracy, including the asymptotic scaling behavior of the isochoric heat capacity in the one- and two-phase regions. Unlike the crossover cubic EOS developed earlier [Fluid Phase. Equilibr. 147 (1998) 7], the GC EOS is based on the crossover sine model and can be extended into the metastable region for representing analytically connected van der Waals loops. In addition, using the GC EOS and the decoupled-mode theory (DMT) we have developed a generalized GC + DMT model, which reproduces the singular behavior of the thermal conductivity of pure fluids in and beyond the critical region. Unlike the DMT model based on the asymptotic crossover equation of state CREOS-97, the GC + DMT model is valid in the entire fluid state region at $T \geq T_b$ (where T_b is the binodal temperature), and at $\rho \to 0$ reproduces the dilute gas contributions for the transport coefficients.

Keywords: Critical region; Crossover theory; Equation of state; Heat capacity; Thermal conductivity; Carbon dioxide; Ethane; Methane; Water

1. Introduction

During the last two decades many efforts have been made to develop a "global", or generalized EOS that at low densities reproduces the ideal gas equation and is transformed into the non-analytic scaled EOS as the critical point is approached [1–27]. The most theoretically advanced models are probably the hierarchical reference theory (HRT) developed by Parola et al. [3–7] and the "globalized" renormalization-group (RG) procedure proposed by White et al. [15–19]. An advantage of the HRT [3–7] and "globalized" RG [15–19] models is that they require only few microscopic intermolecular potential parameters as input. However, they are rather complicated and require additional spline functions for the practical representation of the thermodynamic surface of real fluids. Besides, so far, first-principle theoretical models [3–7,15–19,23–27] have been focused only on reproducing of the VLE and PVT surfaces, but not the singular behavior of the caloric properties, such as the isochoric and isobaric heat capacities.

In this paper we continue a study initiated in our previous works for the crossover cubic EOS [28,29] and thermal conductivity in sub- and super-critical fluids [30–34]. Using the crossover sine model [35], we first develop a generalized cubic (GC) EOS for methane, ethane, carbon dioxide, and water. The new equation of state was tested against an extensive set of experimental data for the volumetric and caloric properties. Unlike the cubic crossover EOS developed previously [28], the GC EOS is based on the crossover sine-model and can be analytically extended into the metastable region and reproduces the asymptotic scaling behavior of the isochoric heat capacity in the one- and two-phase regions. Then we apply the GC EOS for the calculation of the thermal conductivity of methane, ethane, and carbon dioxide with the crossover decoupled-mode model developed by Kiselev and Kulikov [30,32].

We proceed as follows. In Section 2 we develop a generalized cubic EOS for pure fluids. In Section 3 we apply this EOS for the thermodynamic properties in methane, ethane, carbon dioxide, and water. The thermal conductivity calculations are presented in Section 4, and our results are summarized in Section 5.

* Corresponding author. Tel.: +1 303 273 3190; fax: +1 303 273 3730.
E-mail address: skiselev@mines.edu (S.B. Kiselev).

0378-3812/$ – see front matter © 2004 Elsevier B.V. All rights reserved.
doi:10.1016/j.fluid.2004.06.014

2. Generalized cubic EOS

In this work, the Patel–Teja (PT) EOS [36,37]

$$P = \frac{RT}{v-b} - \frac{a(T)}{v(v+b)+c(v-b)} \tag{1}$$

(where P is the pressure, $v = 1/\rho$ is molar volume, and R is the universal gas constant) has been chosen as a reference cubic EOS for one-component fluids. The PT EOS is a good choice for developing a GC EOS because by setting $b = c = 0$ in the attractive term, it is transformed into the vdW EOS. With $b \neq 0$ and $c = 0$ it corresponds to the Redlich–Kwong–Soave (RKS) EOS [38,39], and choosing $b = c \neq 0$ the PT is transformed into the Peng–Robinson (PR) EOS [40]. In the original PT EOS [36,37]

$$a(T) = \Omega_a \frac{R^2 T_{0c}^2}{P_{0c}} \alpha_a(T) = a_{0c}\alpha_a(T),$$
$$b = \Omega_b \frac{R^2 T_{0c}}{P_{0c}}, \qquad c = \Omega_c \frac{RT_{0c}}{P_{0c}}, \tag{2}$$

where

$$\alpha_a(T_r) = 1 + c_1(T_r - 1) + c_2(\sqrt{T_r} - 1) + c_3(T_r^{0.8} - 1) \tag{3}$$

is a function of the dimensionless temperature $T_r = T/T_{0c}$, the coefficients Ω_a, Ω_b, Ω_c are functions of the critical compressibility Z_{0c}, and the classical critical parameters T_{0c}, P_{0c} and v_{0c} that can be found from the condition

$$\left(\frac{\partial P}{\partial v}\right)_{T_{0c}} = 0, \qquad \left(\frac{\partial^2 P}{\partial v^2}\right)_{T_{0c}} = 0,$$
$$\frac{P_{0c}v_{0c}}{RT_{0c}} = Z_{0c} \leq \frac{1}{3}. \tag{4}$$

In order to develop a generalized—"global" crossover EOS, which reproduces the ideal gas equation in the limit of low densities, we will follow the crossover approach developed by Kiselev [28]. Following this approach, we first represent the dimensionless Helmholtz free energy $\bar{A} = A(T, v)/RT$ in the form

$$\bar{A}(T, v) = \Delta\bar{A}(\Delta T, \Delta v) + \bar{A}_{bg}(T, v), \tag{5}$$

where the critical part of the Helmholtz free energy

$$\Delta\bar{A}(\Delta T, \Delta v) = \bar{A}^{res}(\Delta T, \Delta v) - \bar{A}^{res}(\Delta T, 0) - \ln(\Delta v + 1) + \Delta v\bar{P}_0(\Delta T), \tag{6}$$

and the background contribution is given by

$$\bar{A}_{bg}(T, v) = -\Delta v\bar{P}_0(T) + \bar{A}_0^{res}(T) + \bar{A}^{id}(T). \tag{7}$$

In Eqs. (5)–(7), $\Delta T = T/T_{0c} - 1$ and $\Delta v = v/v_{0c} - 1$ are dimensionless distances from the classical critical temperature T_{0c} and molar volume v_{0c}, respectively, $\bar{P}_0(T) = P(T, v_{0c})v_{0c}/RT$ is the dimensionless pressure, $\bar{A}_0^{res}(T) = \bar{A}^{res}(T, v_{0c})$ is the dimensionless residual part of the Helmholtz energy along the critical isochore $v = v_{0c}$, and $\bar{A}^{id}(T)$ is the dimensionless temperature-dependent ideal-gas Helmholtz free energy.

In the next step, we replace the classical values of ΔT and Δv in the critical part $\Delta\bar{A}(\Delta T, \Delta v)$ with the renormalized values

$$\bar{\tau} = \tau\Upsilon^{-\alpha/2\Delta_1},$$
$$\bar{\varphi} = \varphi\Upsilon^{(\gamma-2\beta)/4\Delta_1} + (1+\varphi)\Delta v_c\Upsilon^{(2-\alpha)/2\Delta_1}, \tag{8}$$

where $\alpha = 0.11$, $\beta = 0.325$, $\gamma = 2 - 2\beta - \alpha = 1.24$, and $\Delta_1 = 0.51$ are universal non-classical critical exponents [41,42], $\tau = T/T_c - 1$ is a dimensionless deviation of the temperature from the real critical temperature T_c, $\varphi = v/v_c - 1$ is a dimensionless deviation of the molar volume form the real critical molar volume v_c, $\Delta v_c = (v_c - v_{0c})/v_{0c} \ll 1$ is a dimensionless shift of the critical volume, and $\Upsilon(\tau, \varphi)$ denotes a crossover function. In this work, for $\Upsilon(\tau, \eta)$ we use a simple phenomenological expression obtained by Kiselev et al. [28,29,43]

$$\Upsilon(q) = \left(\frac{q}{1+q}\right)^{2\Delta_1}, \tag{9}$$

where $q = (r/Gi)^{1/2}$ is a renormalized distance to the critical point and $r(\tau, \varphi)$ is a parametric variable. The crossover function Υ given by Eq. (9) coincides with the corresponding crossover function in the CR Leung–Griffiths model obtained in the first order of ε-expansion by Belyakov et al. [44]. In our previous work [28,43], the renormalized distance q was found from a solution of the crossover linear model (LM) [29]. In this study, following our recent work [45] we find q from a solution of the crossover sine model (SM)

$$\left(q^2 - \frac{\tau}{Gi}\right)\left[1 - \frac{p^2}{4b^2}\left(1 - \frac{\tau}{q^2 Gi}\right)\right] = b^2\left\{\frac{\varphi[1 + v_1\exp(-10\varphi)] + d_1\tau}{m_0 Gi^{\beta}}\right\}^2 \Upsilon^{(1-2\beta)/\Delta_1}, \tag{10}$$

where m_0, v_1, d_1, and Gi are the system-dependent parameters, while the universal parameters p^2 and b^2 can be set equal to the linear model (LM) parameter $p^2 = b^2 = b_{LM}^2 = 1.359$ [35]. The crossover SM as given by Eq. (10) is physically equivalent to the crossover sine model developed earlier [35,46,47], but with different empirical term $\propto v_1\exp(-10\varphi)$. The coefficient v_1, which is supposed to be positive and small ($0 \leq v_1 \ll 1$), provides at the triple point of liquids a physically obvious condition $\Upsilon = 1$. In the asymptotic critical and low-density regions this term is negligibly small and the linear-model crossover equation for the parametric variable q employed earlier by Kiselev et al. [48–51] is recaptured from Eq. (10) when parameter $p^2 \to 0$. At $p^2 \neq 0$ and at $q \ll 1$, Eq. (10) is transformed into the

symmetric trigonometric model developed by Fisher et al. [52]. The difference between the trigonometric model developed by Fisher et al. [52] and the crossover SM as given by Eq. (10) in the asymptotic regime $q \to 0$ is only in the definition of the order parameter.

Finally, the crossover expression for the Helmholtz free energy can be written in the form

$$\bar{A}(T, v) = \Delta\bar{A}(\bar{\tau}, \bar{\varphi}) - K(\tau, \varphi) - \Delta v\bar{P}_0(T) + \bar{A}_0^{\mathrm{res}}(T) + \bar{A}_{\mathrm{id}}(T) \quad (11)$$

with the kernel term

$$K(\tau, \varphi) = \tfrac{1}{2}a_{20}\tau^2[\Upsilon^{-\alpha/\Delta_1}(\tau, \varphi) - 1] + \tfrac{1}{2}a_{21}\tau^2[\Upsilon^{-(\alpha-\Delta_1)/\Delta_1}(\tau, \varphi) - 1], \quad (12)$$

where the coefficients a_{20} and a_{21} correspond to the asymptotic and first Wegner-correction terms, respectively. Asymptotically close to the critical point (at $q \ll 1$, or $|\tau| \ll Gi$ at $\rho = \rho_c$ and $|\varphi| \ll Gi^{\beta}$ at $T = T_c$), the crossover function $\Upsilon \propto r^{\Delta_1}$, and the critical part $\Delta\bar{A}$ becomes a non-analytical scaling function of τ and φ, while far away from the critical point (at $q \gg 1$, or $|\tau| \gg Gi$ at $\rho = \rho_c$ and $|\varphi| \gg Gi^{\beta}$ at $T = T_c$) the crossover function $\Upsilon \to 1$ and Eq. (11) is transformed into the classical Helmholtz free energy (5).

The GC EOS can be obtained by differentiation of Eq. (11) with respect to volume

$$P(v, T) = -RT\left(\frac{\partial\bar{A}}{\partial v}\right) = \frac{RT}{v_{0c}}\left\{-\frac{v_{0c}}{v_c}\left[\left(\frac{\partial\Delta\bar{A}}{\partial\varphi}\right)_T - \left(\frac{\partial K}{\partial\varphi}\right)_\tau\right] + \bar{P}_0(T)\right\}. \quad (13)$$

It is easily to show that in the GC EOS with the kernel term as given by Eq. (12) the isochoric heat capacity $C_V = -T(\partial^2 A/\partial T^2)_\rho$ along the critical isochore $\rho = \rho_c$ diverges at $\tau \to 0$ as

$$\frac{C_V(\tau)}{R} = A_0^{\pm}|\tau|^{-\alpha}(1 + a_1^{\pm}|\tau|^{\Delta_1}) + B_0^{\pm}(\tau) \quad (14)$$

where $A_0^{\pm}$, is the asymptotic amplitude, $a_1^{\pm}$ is the first Wegner-correction term [53], and $B_0^{\pm}(\tau)$ is a background contribution above (+) and bellow (−) critical temperature.

3. Thermodynamic properties

For one-component fluids the GC EOS contains six classical system-dependent parameters, namely, the critical parameters T_{0c}, v_{0c}, Z_{0c}, and coefficients c_i (i = 1–3). In addition to the classical parameters, the GC EOS also contains the Ginzburg number Gi, the critical shift Δv_c, the coefficients m_0, v_1, d_1, and the kernel term amplitudes a_{20} and a_{21}. Thus, the crossover Helmholtz free energy for the GC EOS as given by Eq. (11) contains 13 adjustable parameters. In practice, however, the number of the adjustable parameters is less. Since the real critical parameters T_c, P_c, and Z_c for a one-component fluids are usually known, the critical shift $\Delta v_c = v_c/v_{0c} - 1$ is known too. Thus using the conditions $T_{0c} = T_c$ and $P_{0c} = P_c$, one can reduce the number of adjustable parameters to ten: the classical compressibility factor Z_{0c}, the coefficients c_i (i = 1–3), the Ginzburg number Gi, the coefficients m_0, v_1, d_1, and the critical amplitudes a_{20} and a_{21}.

In this work, we tested the GC EOS against experimental data for methane, ethane, carbon dioxide, and water. The classical compressibility factor Z_{0c}, the Ginzburg number Gi, and the coefficients c_i (i = 1–3), m_0, v_1, and d_1 were found from a fit of Eqs. (11)–(13) to experimental VLE- and PVT-data in one and two-phase regions, while the amplitudes a_{20} and a_{21} for all substances have been found from a fit of the GC EOS to the C_V-data along the critical isochore generated asymptotically closed to the critical point at $T \geq T_c$ with the parametric crossover model developed by Kiselev [49] for methane and ethane, by Kiselev and Kulikov [32] for carbon dioxide, and by Kiselev and Friend [54] for water. The system-dependent parameters for the GC EOS for methane, ethane, carbon dioxide and water are listed in Table 1, and comparisons of the predictions of the model with experimental data are shown in Figs. 1–6.

In Fig. 1 we show a comparison of the GC EOS with experimental PVT and VLE data for methane and ethane, and for carbon dioxide and water in Fig. 2. The filled squares in Fig. 2 indicate the VLE data generated for water with the IAPWS-95 Formulation [55]. As one can see, the GC EOS yields a very good representation of the thermodynamic surface of pure fluids in a wide range of state variables, including the critical region. In the region bounded by $0.5\rho_c \leq \rho \leq 1.5\rho_c$ and $T_c \leq T \leq 1.5T_c$ an average absolute deviation (AAD) for pressure is less then 1%, and at $\rho \geq 2\rho_c$ the GC EOS reproduces the liquid densities for all substances with AAD of about 1–2%. For all substances in the temperature region $0.3T_c \leq T \leq T_c$, the GC EOS reproduces the saturated pressure data with an AAD of about 0.5–1%, the liquid density data with an AAD of about 1%, and the vapor density with about 2–3%. For carbon dioxide and water these AAD are approximately the same as in the CR PT EOS developed earlier by Kiselev [28] on the basis of the linear-model (LM) EOS. Although the LM EOS has a theoretical foundation in the renormalization-group theory and was confirmed in the second order of ε-expansion and in high-temperature expansion [56], it cannot be analytically extended deep into the metastable region. This in turn restricts its applications to interface modeling and makes VLE calculations in fluid mixtures extremely unstable [29]. As one can see from Figs. 1 and 2, the GC EOS, unlike the CR EOS based on the LM equation for Υ, can be extended into the metastable region and at temperatures $T < T_c$ represents analytically connected van der Waals loops. The dashed lines in Figs. 1 and 2 represent the values calculated with developed recently the generalized corresponding state (GCS)

Table 1
System-dependent constants for the GC EOS

	CH_4	C_2H_6	CO_2	H_2O
Classical critical parameters				
Z_{0c}	3.333333E−01	3.290717E−01	3.333333E−01	3.030889E−01
T_{0c} (K)	1.905640E+02	3.053220E+02	3.041282E+02	6.470960E+02
ρ_{0c} (mol l^{-1})	8.708152E+00	5.830862E+00	8.752363E+00	1.353034E+01
Critical shift				
Δv_c	−1.39681E−01	−1.50037E−01	−1.76237E−01	−2.44831E−01
Classical PT EOS parameters				
c_1	−1.783195E+01	−7.735786E+00	−8.329461E−01	5.896251E+00
c_2	−3.255994E+01	−1.020609E+01	−1.654726E+00	2.767574E+00
c_3	3.590565E+01	1.516193E+01	9.417602E−01	−1.015037E+01
Crossover parameters				
Gi	1.365464E−01	5.534679E−02	6.399020E−02	5.897337E−02
m_0	1.197025E+00	1.145878E+00	1.444410E+00	1.439207E+00
v_1	5.920748E−02	3.008093E−02	3.138710E−02	2.988727E−03
d_1	−4.087222E−01	9.930443E−01	2.629753E+00	4.325967E+00
a_{20}	1.590924E+01	1.631399E+01	1.585024E+01	1.020517E+01
a_{21}	4.779291E+00	6.462911E−01	−5.333093E−01	−5.252759E+00

model [45], which requires only the critical parameters T_c, P_c, ρ_c, and the accentric factor ω as input. As one can see, in the one-phase region at $T > 0.6T_c$ and $\rho \leq 1.9\rho_c$ the GCS model reproduces the experimental PVT-data practically with the same accuracy as the GC EOS. However, the GCS model, unlike the GC EOS, does not contain the kernel term and is unable to reproduce the correct asymptotic behavior of the isochoric heat capacity in the critical region.

In Figs. 3 and 4 we compare experimental values of the isobaric heat capacities, C_P, with the values calculated with the GC EOS. Since the data shown in Figs. 3 and 4 were not used in optimization procedure, this is a good test of the consistency of the GC EOS. The dotted-dashed curves in Figs. 3 and 4 represent the values calculated with the CREOS-97 [32,49,54]. As one can see, in the asymptotic critical region the CREOS-97 yields a better representation of experimental C_P data than the GC EOS, which predicts systematically lower values than ones calculated with the CREOS-97. This is not surprising, because the parametric crossover model CREOS-97 was specially developed for reproducing of the thermodynamic surface of pure fluids and binary mixtures in the critical region with a high accuracy.

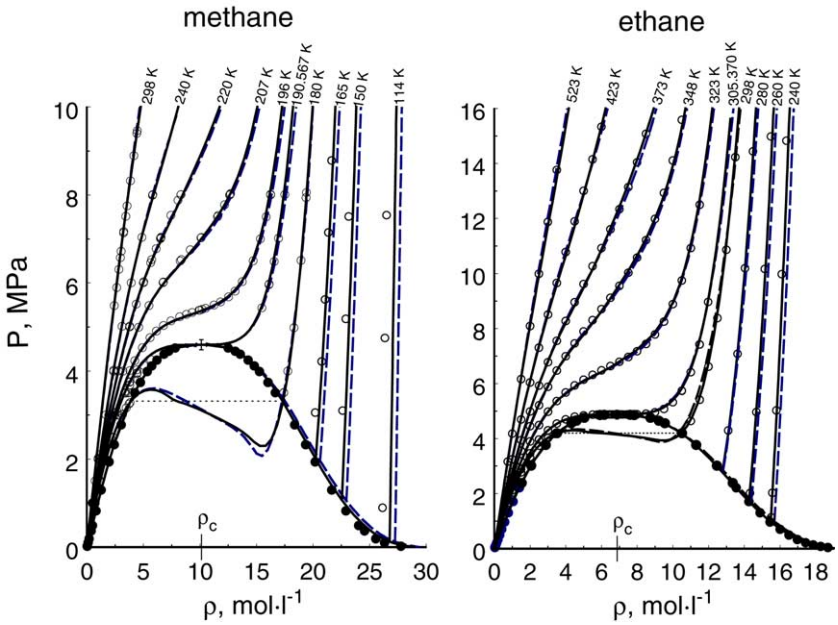

Fig. 1. $P\rho T$ data for methane [68–70] (left) and ethane [71] (right) with predictions of the GC EOS (solid curves) and the GCS model (dashed curves). The empty symbols correspond to the one-phase region and the filled symbols indicate the VLE data.

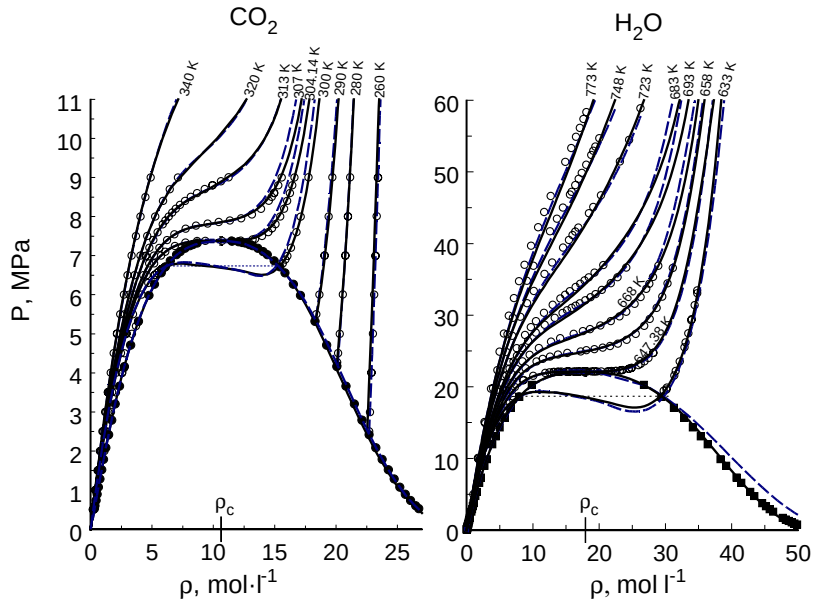

Fig. 2. $P\rho T$ data for carbon dioxide [72,73] (left) and water [74–77] (right) with predictions of the GC EOS (solid curves) and the GCS model (dashed curves). The empty symbols correspond to the one-phase region, and the filled symbols indicate the VLE data.

It is obvious that a simple cubic EOS, even in the crossover formulation, is unable to reproduce the heat capacity data in the critical region with the same accuracy. However, the big deviations of the GC EOS from the CREOS-97 are observed only in the nearest vicinity to the critical point. Outside the asymptotic critical region, the GC EOS describes the experimental C_P-data practically with the same accuracy as the CREOS-97. Except for data-points very close to the critical point, for which deviations increase to 30–40%, the GC EOS reproduces the isobaric heat capacity data shown in Figs. 3 and 4 with AAD of about 2–5% in the low-density region, and with AAD of about 1–2% for liquids.

In Figs. 5 and 6 we show the isochoric heat capacity data along the critical isochore in the two- and one-phase regions in comparison with the predictions of the GC EOS (solid lines) and the CREOS-97 (dotted-dashed lines). As one can see, in the asymptotic critical region the predictions of the GC EOS qualitatively and quantitatively are in a good agreement with experimental data. There are two experimental C_V-data sets for ethane, which are inconsistent with each other in the value of the background contribution to the C_V far from the critical point, where the singular contributions to the C_V are extremely small [57,58]. As one can see from Fig. 5, the experimental data obtained by Shmakov [57,58]

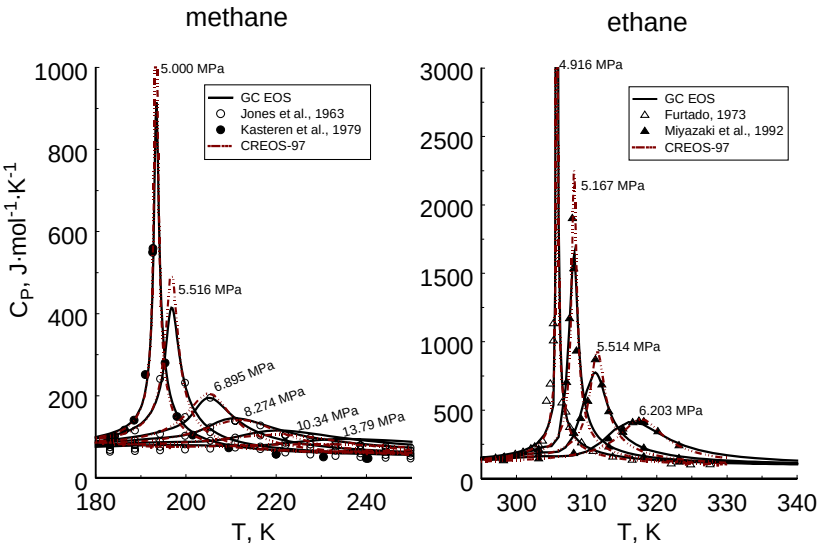

Fig. 3. The isobaric heat capacity data for methane [78,79] (left) and ethane [80,81] (right) with predictions of the GC EOS (solid curves) and the CREOS-97 [49] (dashed curves).

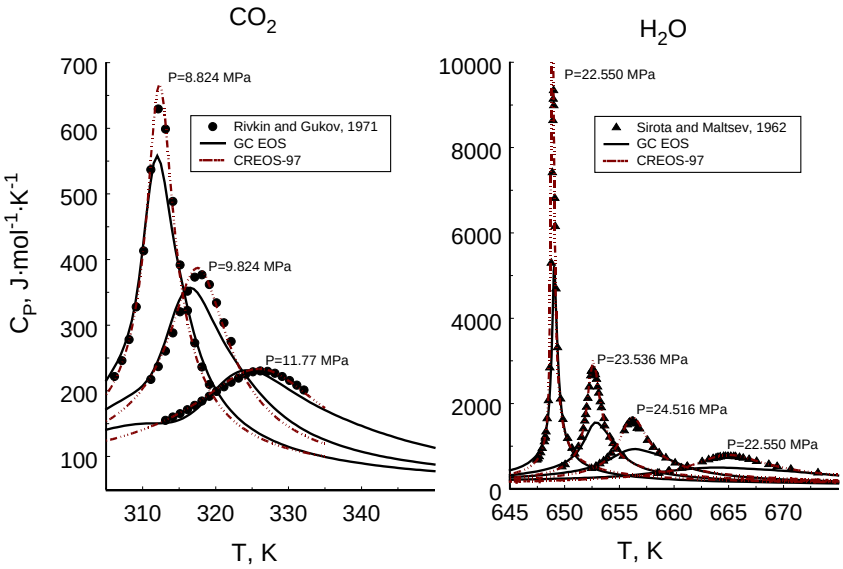

Fig. 4. The isobaric heat capacity data [82] for carbon dioxide (left) and water [83] (right) with predictions of the GC EOS (solid curves) and the CREOS-97 [49] (short dashed curves).

in this region lie systematically lower than experimental values reported by Abdulagatov et al. [57,58]. The CREOS-97 was optimized to the Shmakov's data [57,58], therefore, a good agreement between calculated values and experimental data in the two- and one-phase regions is observed for this model, while the GC EOS is in excellent agreement with experimental data by Abdulagatov et al. [57,58]. Since no experimental data shown in Fig. 5 have been used for the optimization of the GC EOS for ethane, this agreement between experimental data and predicted values of the isochoric heat capacity in the one- and two-phase regions in ethane looks rather impressive. For methane and water the GC EOS predicts in the two-phase region systematically higher values of C_V than experimental data. We need to note that unlike the CREOS-97 [32,49,54], where the reduced density $\Delta\rho = \rho/\rho_c - 1$ is used as the order parameter, in Eqs. (10)–(12) the reduced molar volume $\varphi = v/v_c - 1$ has been chosen as the order parameter. In this case, as it is discussed elsewhere [45,59], in the GC EOS the derivative $(\partial^2 P/\partial T^2)_\rho$ remains finite at the critical point and the divergence of C_V

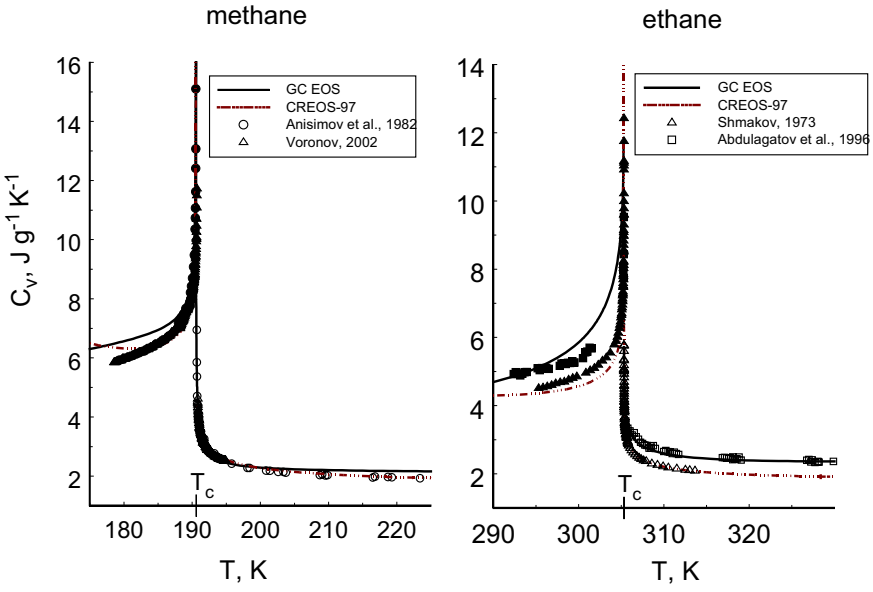

Fig. 5. The isochoric heat capacity data along the critical isochore for methane [84,85] (left) and ethane [57,58] (right) with predictions of the GC EOS (solid curves) and the CREOS-97 [49] (dashed curves). The empty symbols correspond to the one-phase region, and the filled symbols indicate the VLE data.

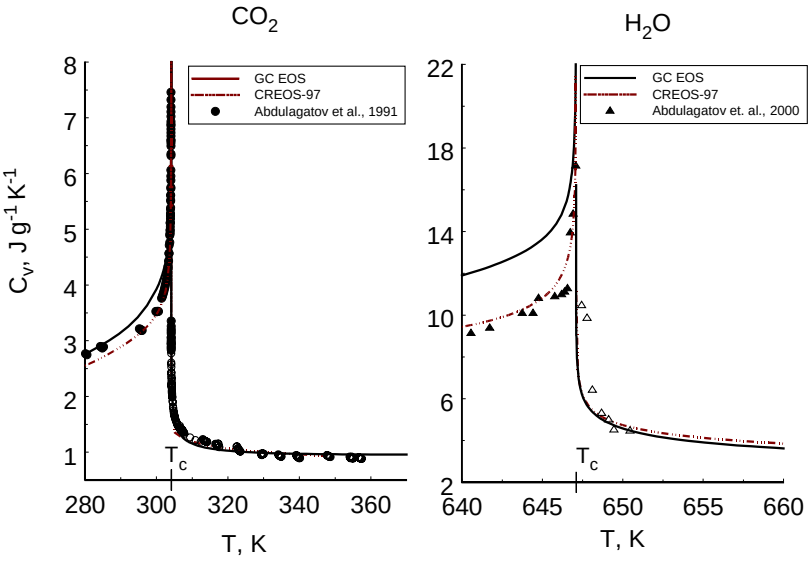

Fig. 6. The isochoric heat capacity data along the critical isochore for carbon dioxide [86] (left) and water [87] (right) with predictions of the GC EOS (solid curves) and the CREOS-97 for CO_2 [32] and H_2O [54] (dashed curves). The empty symbols correspond to the one-phase region, and the filled symbols indicate the VLE data.

along the critical isochore related to the divergence of the second derivative of the chemical potential with respect to the temperature, $(\partial^2\mu/\partial T^2)_{\rho_c(\tau\to 0)} \propto \tau^{-\alpha}$. In spite of this difference in definition of the order parameters, the GC EOS yields a sufficiently accurate representation of the isochoric and isobaric heat capacities in pure fluids that allows us to use the GC EOS for thermal conductivity calculations in the critical region.

4. Thermal conductivity

In this work, for the calculation of the thermal conductivity in the critical region we use a crossover decoupled-mode theory (DMT) model for the transport coefficients in pure fluids and fluid mixtures developed by Kiselev and Kulikov [30,32]. In the limit of pure components, the crossover expression for the thermal conductivity takes the form [33,34]

$$\lambda = \frac{k_B T \rho C_P}{6\pi\eta\hat{\xi}}\Omega(z) + \lambda_b, \tag{15}$$

where k_B is the Boltzmann's constant, η the shear viscosity, λ_b is a background part of the thermal conductivity which is an analytic function of the temperature and density. The crossover function $\Omega(z) = \Omega(q_D\hat{\xi})$ is given by

$$\Omega(z) = \frac{2}{\pi}\left[\tan^{-1}(z) - \frac{1}{\sqrt{1+y_{1D}z}}\tan^{-1}\left(\frac{z}{\sqrt{1+y_{1D}z}}\right)\right] \tag{16}$$

with

$$y_{1D} = \frac{6\pi\eta^2}{k_B T\rho q_D(\phi_1 + y_1^{-1})}, \qquad y_1 = \frac{k_B T\rho C_P}{6\pi\eta\hat{\xi}\lambda_b}. \tag{17}$$

In Eqs. (15)–(17), q_D is a cutoff wave number, $\phi_1 = \phi(k_{1D}\hat{\xi})$ is the dynamical scaling function [33,34]

$$\phi(z) = \frac{3[1+z^2+(z^3-z^{-1})\tan^{-1}(z)]}{4z^2(1+z^2)} \tag{18}$$

calculated at the constant value of the wave number $k_{1D} = 0.1q_D$, and the renormalized correlation length is given by [33]

$$\hat{\xi} = \xi_{OZ}\exp\left(-\frac{1}{q_D\xi_{OZ}}\right), \qquad \xi_{OZ} = \xi_0\sqrt{\frac{\chi_T}{\Gamma_0}}. \tag{19}$$

In Eq. (19), ξ_{OZ} corresponds to the Onrstein–Zernike approximation for the correlation length, and ξ_0 and Γ_0 are the amplitudes of the asymptotic power laws for the correlation length and reduced isothermal compressibility $\chi_T = \rho T(\partial\rho/\partial P)_T P_c\rho_c^{-2}T_c^{-1}$, respectively. Asymptotically close to the critical point (at $q_D\hat{\xi} \gg 1$) the singular part of the thermal conductivity is much larger than the background part ($y_1 \gg 1$, $y_{1D} \approx 1$), the crossover function $\Omega(z)$ approaches unity, and the thermal conductivity along the critical isochore at $T \geq T_c$ diverges as $\lambda \propto \tau^{-\gamma/2}$. Far away from the critical point at $q_D\hat{\xi} \ll 1$ the crossover function $\Omega(z) \to 0$, and the thermal conductivity λ becomes equal to its background part λ_b.

In this work, following Kiselev and Huber [33] we represent the shear viscosity η and background part λ_b as sums of two terms

$$\eta(T,\rho) = \eta_0(T) + \eta_{ex}(T,\rho), \tag{20}$$

$$\lambda_b(T,\rho) = \lambda_0(T) + \lambda_{ex}(T,\rho), \tag{21}$$

where the subscripts "0" and "ex" denote the temperature-dependent dilute gas contributions and the temperature and

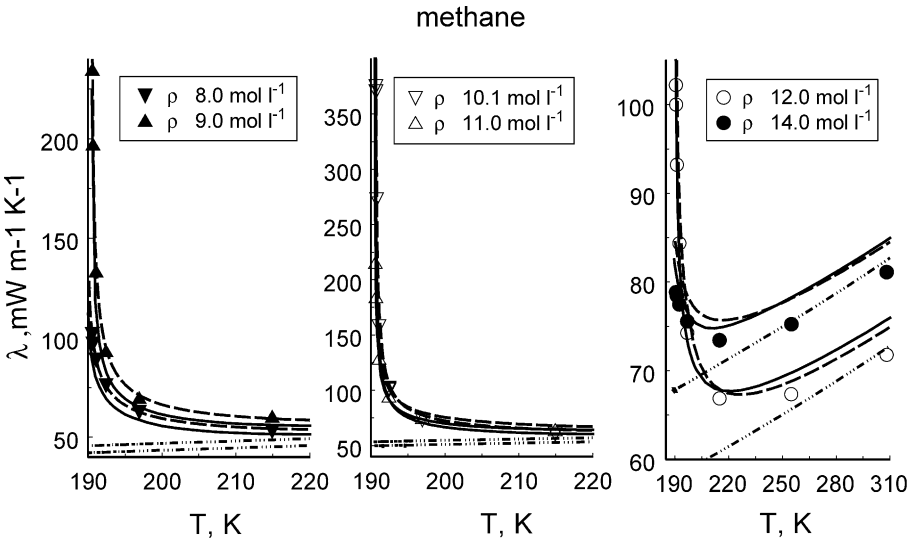

Fig. 7. The thermal conductivity data along the isochores for methane [60] (symbols) with predictions of the GC + DMT model (solid curves) and the CREOS-97 [33] (dashed curves). The dotted-dashed curves correspond to the background contributions calculated at the same isochores.

density dependent excess contributions, respectively. In this work, for $\eta_0(T)$, $\lambda_0(T)$, $\eta_{ex}(T, \rho)$, $\lambda_{ex}(T, \rho)$ and we use the same correlations as described by Kiselev and Huber [33] (see Eqs. (48)–(54) in Ref. [33]). For the parameters ξ_0 and q_D for methane, ethane, and carbon dioxide we also adopted the same values as employed earlier by Kiselev and Huber [33] (see Table 1 in Ref. [33]), while for the calculation of the thermodynamic properties in Eqs. (15)–(19), instead the CREOS-97 model employed in Ref. [33], we use here the GC EOS developed in this work. A comparison of the calculated values of the thermal conductivity with experimental data for methane, ethane, and carbon dioxide is shown in Figs. 7–9.

In Fig. 7, we show the GC + DMT model predictions for the thermal conductivity along the near critical isochores in methane compared with experimental data by Sakonidou [60]. The dashed curves in Fig. 7 represents the values calculated with the asymptotic crossover model, CREOS-97, by Kiselev and Huber [33], and the dotted-dashed curves correspond to the background contributions calculated along the same isochores with Eq. (21). As one can see, in agreement with experimental data both, the GC + DMT and CREOS-97 models yield an anomalous increase in the thermal conductivity in the critical region, while far away from the critical point they reduce to the background contribution given by Eq. (21). A comparison of the thermal conductivity

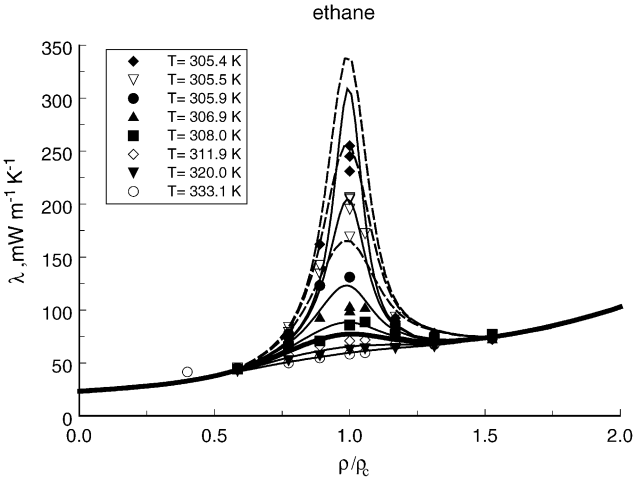

Fig. 8. The thermal conductivity data along the isotherms for ethane [61] (symbols) with predictions of the GC + DMT model (solid curves). The dashed curves represent the values calculated at the first three isotherms (T = 305.4, 305.5, and 305.9 K, respectively) with the CREOS-97 [33].

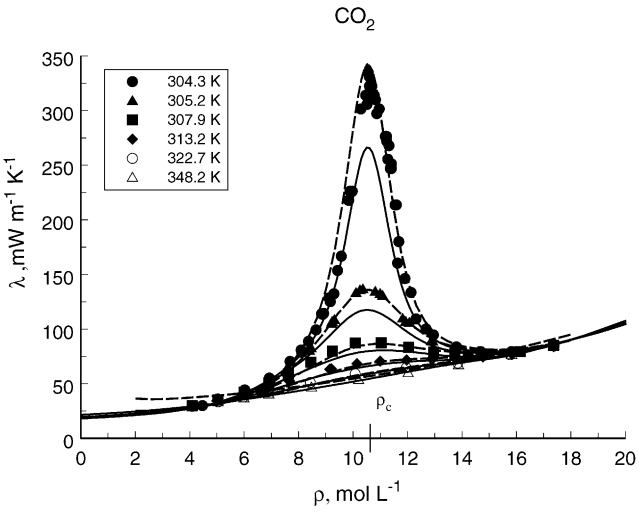

Fig. 9. The thermal conductivity data along the isotherms for carbon dioxide [62] with predictions of the GC + DMT model (solid curves) and the CREOS-97 [33] (dashed curves).

data obtained along the near critical isotherms by Mostert [61] for ethane and by Michels et al. [62] for carbon dioxide with the predictions of the GC + DMT and CREOS-97 [33] models is shown in Figs. 8 and 9. As mentioned above (see Figs. 3 and 4), asymptotically close to critical point the GC EOS gives systematically lower values of the isobaric heat capacity than the CREOS-97. As a consequence, in this region the GC + DMT model also predicts slightly smaller values of the thermal conductivity than ones calculated with the CREOS-97 model [33]. However, we note that the CREOS-97 is an asymptotic crossover model, which is valid only for $\rho \geq 0.25$ [33]. Since the CREOS-97 does not reproduce the ideal gas limit, it may even give unphysical behavior as $\rho \to 0$. The GC + DMT model not only qualitatively, but also quantitatively reproduces the singular behavior of the thermal conductivity of pure fluids in the critical region, and as $\rho \to 0$ gives the dilute gas contribution $\lambda_0(T)$.

5. Conclusion

The advantage of the van der Waals (vdW) [63] and other cubic equations of states [64] is that they contain a restricted number of the molecular parameters, which have a real physical meaning and do not depend on the thermodynamic conditions. However, it is well known that an accuracy of representation of the thermodynamic surface in real fluids with these vdW-type analytical EOS is rather pure, especially in the critical region, where the thermodynamic properties of fluids exhibit the non-analytic, singular behavior. An example of the empirical attempt to improve the representation of the VLE and PVT surface of one-component fluids in the critical region with the simple cubic and non-cubic EOS was presented recently in Refs. [65,66]. The authors of this work, instead following a theoretically well-established procedure, try to achieve their goal by incorporating additional empirical correction terms to a reference EOS. Of course, incorporation of the additional terms will make the resulted EOS more accurate, but certainly not physically self-consistent. As a consequence of the unphysical nature of the correction terms, its number becomes too big (nineteen in Eq. (1) in Ref. [66]), they are loosing their physical meaning, and a rather complicated structure of the "improved" EOS becomes its disadvantage over other short, but more accurate structure optimized empirical EOS [67]. Besides, even with additional empirical near-critical correction terms the "improved" EOS fails to reproduce the singular behavior of the isochoric heat capacity in the vicinity of the critical point. In the critical region fluids exhibit a universal singular behavior, which is determined by the interaction of the enormously big fluctuations of the order parameter, or the density for one-component fluids. All analytical and non-analytical terms introduced in Refs. [65,66] have nothing to do with the critical fluctuations and, therefore, cannot result in the non-analytic singular behavior of the isochoric heat capacity in the critical region. In order to incorporate the critical fluctuations into the equation of state, the more rigorous theoretical approaches should be considered.

A general approach for developing a generalized crossover EOS, which in the critical region reproduces theoretically well-established scaling laws, and in the limit of low densities is transformed into the ideal gas equation was proposed by Kiselev [28]. In our previous work [45], we used this approach for developing a generalized corresponding states model (GCSM), which contains the critical point parameters and accentric factor as input, but reproduces the PVT- and VLE-surface and the surface tension of one-component fluids (polar and non-polar) with high accuracy. However, since the kernel term in the GCSM was set equal to zero, the singular behavior of the isochoric heat capacity was not considered in Ref. [45]. In this work, using the Patel–Teja (PT) EOS [36] as a reference EOS for one-component fluids, we developed a generalized cubic EOS for methane, ethane, carbon dioxide, and water. The GC EOS contains 10 adjustable parameters and at $T \geq T_c$ and reproduces the pressures with an average absolute deviation (AAD) less then 1%, and liquid densities at $\rho \geq 2\rho_c$ with AAD of about 1–2%. In the temperature region $T \leq T_c$, the GC EOS reproduces the saturated pressure data with AAD of about 0.5–1%, the liquid density data with AAD of about 1%, and the vapor density with about 2–3%. Unlike the cubic crossover EOS developed before [28], the new sine-model based GC EOS can be analytically extended into the metastable and unstable regions and is capable of reproducing the asymptotic scaling behavior of the isochoric heat capacity in the one- and two-phase regions. This allowed us to develop a generalized GC + DMT model for the transport coefficients in pure fluids based on the GC EOS and the decoupled-mode theory by Kiselev and Kulikov [30,32]. Unlike the asymptotic crossover model CREOS-97 developed earlier by Kiselev and Huber [33], the GC + DMT model is valid in the entire fluid state region $T \geq T_b$, where T_b is the temperature along the binodal and at $\rho \to 0$ reproduces the dilute gas contributions for the transport coefficients.

We are not aware of any other empirically "improved" cubic or non-cubic EOS, which is able of reproducing the thermodynamic and transport properties of pure fluids in and beyond the critical region with the same accuracy and physical self-consistency. Therefore, we consider the results presented in this work as an additional proof of a general statement that improvements of the description of the critical region with a statistical fluid theory-based EOS can be achieved not by adding empirical analytical and non-analytical terms in these equations, but rather applying to them the more rigorous, renormalization group theory-based methods.

List of symbols

a	temperature-dependent parameter in Eq. (1)
a_{2i}	system-dependent parameter in Eq. (12) ($i = 0, 1$)
A	Helmholtz free energy

$\bar{A}$	dimensionless Helmholtz free energy
$\bar{A}_0$	dimensionless ideal gas part of free energy
$\bar{A}_0^{\mathrm{res}}$	dimensionless ideal residual part along the critical isochore
b	temperature-independent parameter in Eq. (1)
b_2	universal linear-model parameter in Eq. (10)
c	temperature-independent parameter in Eq. (1)
c_i	system-dependent coefficients in Eq. (3) ($i = 1$–3)
C_P	isobaric heat capacity
C_V	isochoric heat capacity
d_1	system-dependent coefficient in Eq. (10)
g	inverse Ginzburg number
Gi	Ginzburg number
k_{B}	Boltzmann's constant
K	kernel term
m_0	system-dependent coefficients in Eq. (10)
M_{w}	molecular weight
p^2	universal sine-model parameter in Eq. (10)
P	pressure (MPa)
P_{c}	critical pressure (MPa)
$\bar{P}_0$	dimensionless pressure along the critical isochore
q	argument of the crossover function
q_{D}	cutoff wave number
R	gas constant
T	temperature (K)
T_{c}	critical temperature (K)
v	molar volume ($\mathrm{l\,mol^{-1}}$)
v_{c}	critical volume ($\mathrm{l\,mol^{-1}}$)
v_1	system-dependent coefficient in Eq. (10)
z	argument of the dynamical crossover function
Z_{c}	critical compressibility factor

Greek letters

α	universal critical exponent
α_{a}	temperature-dependent function in Eq. (2)
β	universal critical exponent
γ	universal critical exponent
Γ_0	critical amplitude
Δ	difference
Δ_1	universal critical exponents
η	shear viscosity
λ	thermal conductivity
ξ	correlation length
ξ_0	critical amplitude
ρ	molar density ($\mathrm{mol\,l^{-1}}$)
τ	reduced temperature difference
$\bar{\tau}$	renormalized temperature difference
Υ	crossover function
ϕ_1	dynamical scaling function
φ	order parameter
$\bar{\varphi}$	renormalized order parameter
Ω	dynamical crossover function in Eq. (15)
Ω_x	dimensionless parameters in Eq. (2) ($x \in a, b, c$)

Subscripts

bg, b	background
c	critical
ex	excess
OZ	Onrstein–Zernike
0	classical

Superscripts

id	ideal gas part
res	residual

Acknowledgements

The authors are indebted to I.M. Abdulagatov for providing us with the original experimental data for *n*-alkanes obtained in the Dagestan Scientific Center of the Russian Academy of Science, and to V.P. Voronov for providing us with his unpublished experimental C_V-data for methane. The research was supported by the US Department of Energy, Office of Basic Energy Sciences, under the Grant No. DE-FG03-95ER14568.

References

[1] J.R. Fox, Fluid Phase Equilibr. 14 (1983) 45–53.
[2] J.R. Fox, T.S. Strovick, Int. J. Thermophys. 11 (1990) 61–72.
[3] A. Parola, L. Reatto, Phys. Rev. Lett. 53 (1984) 2417–2420.
[4] A. Parola, L. Reatto, Phys. Rev. A 31 (1985) 3309–3322.
[5] A. Parola, A. Meroni, L. Reatto, Int. J. Thermophys. 10 (1989) 345–356.
[6] M. Tau, A. Parola, D. Pini, L. Reatto, Phys. Rev. E 52 (1995) 2644–2655.
[7] L. Reatto, A. Parola, J. Phys.: Condens. Matter 8 (1996) 9221–9231.
[8] D. Pini, A. Parola, L. Reatto, Int. J. Thermohys. 19 (1998) 1545.
[9] D. Pini, G. Stell, N.B. Wilding, Mol. Phys. 95 (1998) 483.
[10] P.C. Albright, J.V. Sengers, J.F. Nicoll, M. Ley-Koo, Int. J. Thermophys. 7 (1986) 75–85.
[11] A. Kostrowichka Wyszalkovska, M.A. Anisimov, J.V. Sengers, Fluid Phase Equilibr. 158–160 (1999) 523–535.
[12] A. van Pelt, G.X. Jin, J.V. Sengers, Int. J. Thermophys. 15 (1994) 687–697.
[13] D.D. Erikson, T.W. Leland, Int. J. Thermophys. 7 (1986) 911.
[14] J.J. De Pablo, J.M. Prausnitz, Fluid Phase Equilibr. 59 (1990) 1.
[15] J.A. White, S. Zhang, J. Chem. Phys. 103 (1990) 1922.
[16] J.A. White, S. Zhang, J. Chem. Phys. 99 (1993) 2012.
[17] J.A. White, J. Chem. Phys. 111 (1999) 9352.
[18] J.A. White, J. Chem. Phys. 112 (2000) 3236.
[19] J.A. White, Int. J. Thermophys. 22 (2001) 1147–1157.
[20] T. Kraska, U.K. Deiters, Int. J. Thermophys. 15 (1994) 261–281.
[21] T. Kraska, J. Supercrit. Fluids 16 (1999) 1.
[22] Y. Tang, J. Chem. Phys. 109 (1998) 5935–5944.
[23] L. Lue, J.M. Praustitz, J. Chem. Phys. 108 (1998) 5529–5536.
[24] L. Lue, J.M. Praustitz, AIChE J. 44 (1998) 1455–1466.
[25] F. Fornasiero, L. Lue, A. Bertucco, AIChE J. 45 (1999) 906–915.
[26] J. Jiang, J.M. Prausnitz, J. Chem. Phys. 111 (1999) 5964.
[27] J. Jiang, J.M. Prausnitz, Fluid Phase Equilibr. 169 (2000) 127–147.
[28] S.B. Kiselev, Fluid Phase Equilibr. 147 (1998) 7–23.
[29] S.B. Kiselev, D.G. Friend, Fluid Phase Equilibr. 162 (1999) 51–82.
[30] S.B. Kiselev, V.D. Kulikov, Int. J. Thermophys. 15 (1994) 283–308.

[31] S.B. Kiselev, A.A. Povodyrev, High Temp. 34 (1996) 621–639.
[32] S.B. Kiselev, V.D. Kulikov, Int. J. Thermophys. 18 (1997) 1143–1179.
[33] S.B. Kiselev, M.L. Huber, Fluid Phase Equilibr. 142 (1998) 253–280.
[34] S.B. Kiselev, R.A. Perkins, M.L. Huber, Int. J. Refrig. 22 (1999) 509–520.
[35] S.B. Kiselev, J.F. Ely, Fluid Phase Equilibr. 174 (2000) 93–119.
[36] N.C. Patel, A.S. Teja, Chem. Eng. Sci. 37 (1982) 463–473.
[37] N.C. Patel, Int. J. Thermophys. 17 (1996) 673–680.
[38] O. Redlich, J.N.S. Kwong, Chem. Rev. 44 (1949) 233.
[39] G. Soave, Chem. Eng. Sci. 27 (1972) 1197.
[40] D.Y. Peng, D.B. Robinson, Ind. Eng. Chem. Fundam. 15 (1976) 59.
[41] J.V. Sengers, J.M.H. Levelt Sengers, Annu. Rev. Phys. Chem. 37 (1986) 189–222.
[42] M.A. Anisimov, S.B. Kiselev, in: A.E. Scheindlin, V.E. Fortov (Eds.), Thermal Physics Reviews, vol. 3, Part 2, Harwood Academic, New York, 1992, pp. 1–121.
[43] S.B. Kiselev, J.F. Ely, Ind. Eng. Chem. Res. 38 (1999) 4993–5004.
[44] M.Y. Belyakov, S.B. Kiselev, J.C. Rainwater, J. Chem. Phys. 107 (1997) 3085–3097.
[45] S.B. Kiselev, J.F. Ely, J. Chem. Phys. 119 (2003) 8645–8662.
[46] S.B. Kiselev, J.F. Ely, H. Adidharma, M. Radosz, Fluid. Phase. Equilibr. 183/184 (2000) 53–64.
[47] S.B. Kiselev, J.F. Ely, I.M. Abdulagatov, J.W. Magee, Int. J. Thermophys. 6 (2000) 1373–1405.
[48] S.B. Kiselev, J.V. Sengers, Int. J. Thermophys. 14 (1993) 1–32.
[49] S.B. Kiselev, Fluid Phase Equilibr. 128 (1997) 1–28.
[50] S.B. Kiselev, J.C. Rainwater, J. Chem. Phys. 109 (1998) 643–657.
[51] S.B. Kiselev, High Temp. 28 (1990) 42–49.
[52] M. Fisher, S.-Y. Zinn, P. Upton, Phys. Rev. B 59 (1999) 14533–14545.
[53] F.J. Wegner, Phys. Rev. B 5 (1972) 4529–4536.
[54] S.B. Kiselev, D.G. Friend, Fluid Phase Equilibr. 155 (1999) 33–55.
[55] Release of the IAPWS Formulation 1995 for the Thermodynamic Properties of Ordinary Water Substance for General and Scientific Use, Frederica, Denmark, 1996.
[56] M. Campostrini, A. Pelisseto, P. Rossi, E. Vicari, Phys. Rev. E 60 (1999) 3526–3563.
[57] N.G. Shmakov, Teplofiz. Svoistva Veschestv Mater. (USSR) 7 (1973) 155.
[58] I.M. Abdulagatov, S.B. Kiselev, L.N. Levina, Z.R. Zakaryeva, O.N. Mamchenkova, Int. J. Thermophys. 17 (1996) 423–440.
[59] A. Kostrowicka Wyszalkovska, J.V. Sengers, M.A. Anisimov, Physica A 334 (2004) 482–512.
[60] E.P. Sakonidou, Thermal conductivity of fluids and fluid mixtures in the critical region, Ph.D. Thesis, University of Amsterdam, Amsterdam, 1990.
[61] R. Mostert, The thermal conductivity of ethane and its mixtures with carbon dioxide in the critical region, Ph.D. Thesis, University of Amsterdam, Amsterdam, 1992.
[62] A. Michels, J.V. Sengers, P.S. van der Gulik, Physica 28 (1962) 1216.
[63] J.D. van der Waals, F. Kohnstamm Lehrbuch der Thermostatic, 2er Teil, Verlag von Johann Amrosius Barth, Leipzing, 1927.
[64] A. Anderko, Cubic and generalized van der Waals, in: J.V. Sengers, et al. (Eds.), Equations of State for Fluids and Fluid Mixtures, Part I, Elsevier, Amsterdam, 2000, pp. 75–126.
[65] C.J. Kedge, M.A. Trebble, Fluid Phase Equilibr. 194–197 (2002) 401–409.
[66] C.J. Kedge, M.A. Trebble, Fluid Phase Equilibr. 215 (2004) 91–96.
[67] Span Multiparameter Equations of State—An Accurate Source of Thermodynamic Property Data, Springer-Verlag, Berlin, 2000.
[68] R. Kleinrahm, W. Duschek, W. Wagner, J. Chem. Thermodyn. 18 (1986) 1103.
[69] R. Kleinrahm, W. Duschek, W. Wagner, J. Chem. Thermodyn. 24 (1992) 685.
[70] A. Van Itterbeek, O. Verbeke, K. Staes, Physica 29 (1963) 742.
[71] D.R. Douslin, R.H. Harrison, J. Chem. Thermodyn. 5 (1973) 491.
[72] W. Duschek, R. Kleinrahm, W. Wagner, J. Chem. Thermodyn. 22 (1990) 827–841.
[73] R. Gilgen, R. Kleinrahm, W. Wagner, J. Chem. Thermodyn. 24 (1992) 1243.
[74] S.L. Rivkin, T.S. Akhundov, Teploenergetika 9 (1962) 57.
[75] S.L. Rivkin, T.S. Akhundov, Teploenergetika 10 (1963) 66.
[76] S.L. Rivkin, G.V. Troyanovskaya, Teploenergetika 11 (1964) 72.
[77] S.L. Rivkin, T.S. Akhundov, E.A. Kremenevskaya, N.N. Asadullaeva, Teploenergetika 13 (1966) 59.
[78] M.L. Jones, D.T. Mage, R.C. Faulkner, D.L. Katz, Chem. Eng. Prog. Symp. Ser. 59 (1963) 52.
[79] P.H.G. van Kasteren, Ind. Eng. Chem. Fundam. 18 (1979) 333.
[80] A. Furtado, Ph.D. Thesis, University of Michigan, Ann Arbor, MI, 1973.
[81] T. Miyazaki, A.V. Hejmadi, J.E. Powers, J. Chem. Thermodyn. 12 (1980) 105.
[82] S.L. Rivkin, V.M. Gukov, Teploenergetika 18 (1971) 82.
[83] A.M. Sirota, B.K. Maltsev, Teploenergetika 1 (1962) 52.
[84] M.A. Anisimov, V.G. Beketov, V.P. Voronov, V.B. Nagaev, V.A. Smirnov, Teplofiz. Svoistva Veschestv Mater. (USSR) 16 (1982) 124–135.
[85] V.P. Voronov, Private communication, 2002.
[86] I.M. Abdulagatov, N.G. Polikhronidi, R.G. Batyrova, J. Chem. Thermodyn. 26 (1994) 1031–1045.
[87] I.M. Abdulagatov, V.I. Dvoryanchikov, M.M. Aliev, A.N. Kamalovm, in: P.R. Tremaine, P.G. Hill, D.E. Irish, P.V. Balakrishnam (Eds.), Proceedings of the 13th International Conference on the Properties of Water and Steam, NRC Research Press, Toronto, Canada, 2000, pp. 157–164.